Global marine plankton functional typebiomass distributions: coccolithophores

Working Paper

Author(s):
O'Brien, Colleen; Peloquin, Jill A.; Vogt, Meike; Heinle, Moritz; Gruber, Nicolas [iD]; Ajani, Penelope; Andruleit, Harald; Arístegui, Javier; Beaufort, Luc; Estrada, Marta; Karentz, Deneb; Kopczyńska, Elżbieta; Lee, Renee; Pritchard, Tim; Widdicombe, Claire

Open Access

Earth System
Science
Data

Discussions

Global marine plankton functional type biomass distributions: coccolithophores

C. J. O'Brien[1,*], J. A. Peloquin[1,*], M. Vogt[1], M. Heinle[2], N. Gruber[1], P. Ajani[3], H. Andruleit[4], J. Arístegui[5], L. Beaufort[6], M. Estrada[7], D. Karentz[8], E. Kopczyńska[9], R. Lee[10], T. Pritchard[11], and C. Widdicombe[12]

[1]Environmental Physics Group, Institute for Biogeochemistry and Pollutant Dynamics, ETH Zürich, Universitätsstrasse 16, 8092 Zürich, Switzerland
[2]Laboratory for Global Marine and Atmospheric Chemistry, School of Environmental Sciences, University of East Anglia, Norwich, NR4 7TJ, UK
[3]Department of Biological Sciences, Macquarie University, North Ryde, NSW, 2109, Australia
[4]Bundesanstalt für Geowissenschaften und Rohstoffe (BGR), Geozentrum Hannover, Stilleweg 2, 30655 Hannover, Germany
[5]Instituto de Oceanografía y Cambrio Global (IOCAG), Universidad de Las Palmas de Gran Canaria, 35017, Las Palmas de Gran Canaria, Spain
[6]Centre Européen de Recherche et d'Enseignement des Géosciences de l'Environnement (CEREGE), Europôle Méditerranéen de l'Arbois, Avenue Louis Philibert, BP 80, 13545 Aix en Provence, Cedex 04, France
[7]Institut de Ciencies del MAR (CSIC), Passeig Maritim de la Barceloneta, 3749, 08003 Barcelona, Catalunya, Spain

ESSDD

5, 491–520, 2012

Coccolithophore biomass distributions

C. J. O'Brien et al.

Title Page

Abstract | Instruments

Data Provenance & Structure

Tables | Figures

|◀ | ▶|

◀ | ▶

Back | Close

Full Screen / Esc

Printer-friendly Version

Interactive Discussion

[8]University of San Francisco, College of Arts and Sciences, 2130 Fulton Street, San Francisco, CA 94117, USA
[9]Department of Polar Research, Institute of Ecology, Polish Academy of Sciences, Dziekanow Lesny, 05-092 Lomianki, Poland
[10]Centre for Environmental Science, EPA Victoria, Ernest Jones Drive, Macleod VIC 3085, Australia
[11]Waters and Coastal Science Section, Office of Environment and Heritage, P.O. Box A290, Sydney South NSW 1232, Australia
[12]Plymouth Marine Laboratory, Prospect Place, The Hoe, Plymouth PL1 3DH, UK
[*]These authors contributed equally to this work.

Correspondence to: C. J. O'Brien (colleen.obrien@env.ethz.ch)

Coccolithophore biomass distributions

C. J. O'Brien et al.

Title Page

| Abstract | Instruments |

Data Provenance & Structure

| Tables | Figures |

| I◀ | ▶I |

| ◀ | ▶ |

| Back | Close |

Full Screen / Esc

Printer-friendly Version

Interactive Discussion

Abstract

Coccolithophores are calcifying marine phytoplankton of the class Prymnesiophyceae. They are considered to play an import role in the global carbon cycle through the production and export of organic carbon and calcite. We have compiled observations of global coccolithophore abundance from several existing databases as well as individual contributions of published and unpublished datasets. We estimate carbon biomass using standardised conversion methods and provide estimates of uncertainty associated with these values. The database contains 58 384 individual observations at various taxonomic levels. This corresponds to 12 391 observations of total coccolithophore abundance and biomass. The data span a time period of 1929–2008, with observations from all ocean basins and all seasons, and at depths ranging from the surface to 500 m. Highest biomass values are reported in the North Atlantic, with a maximum of 501.7 $\mu g \, C \, l^{-1}$. Lower values are reported for the Pacific (maximum of 79.4 $\mu g \, C \, l^{-1}$) and Indian Ocean (up to 178.3 $\mu g \, C \, l^{-1}$). Coccolithophores are reported across all latitudes in the Northern Hemisphere, from the Equator to 89° N, although biomass values fall below 3 $\mu g \, C \, l^{-1}$ north of 70° N. In the Southern Hemisphere, biomass values fall rapidly south of 50° S, with only a single non-zero observation south of 60° S. Biomass values show a clear seasonal cycle in the Northern Hemisphere, reaching a maximum in the summer months (June–July). In the Southern Hemisphere the seasonal cycle is less evident, possibly due to a greater proportion of low-latitude data. The original and gridded datasets can be downloaded from Pangaea (http://doi.pangaea.de/10.1594/PANGAEA.785092).

1 Introduction

Marine plankton are the main driver for the global marine cycling of elements such as carbon, nitrogen and phosphorus, primarily through the process of carbon fixation and nutrient uptake during primary production and subsequent export of organic

matter to the deep ocean. Modern marine ecosystem models seek to represent the functional diversity of marine plankton using the concept of Plankton Functional Types (PFTs, Iglesias-Rodríguez, 2002; Le Quéré et al., 2005). PFTs are groups of plankton with defined biogeochemical functions, for example calcification, DMS-production or

5 nitrogen fixation. The inclusion of these groups in marine ecosystem models provides great potential for improving our understanding of marine processes (see for example Dutkiewicz et al., 2012; Marinov et al., 2010; Vogt et al., 2010; Manizza et al., 2010), but has also highlighted a need for extensive observational datasets for model parameterisation and validation (Hood et al., 2006; Le Quéré et al., 2005; Anderson, 2005).

10 The MARine Ecosystem DATa (MAREDAT) project (as part of the MARine Ecosystem Model Intercomparison Project – MAREMIP) seeks to compile global biomass data for PFTs commonly represented in marine ecosystem models: silicifiers, calcifiers (including coccolithophores, pteropods and foraminifera), DMS-producers, picophytoplankton, diazotrophs, bacteria, and three zooplankton sizeclasses (micro-,

15 meso- and macrozooplankton). A summary of the findings for all groups is presented in Buitenhuis et al. (2012).

This paper presents a database of global coccolithophore biomass distributions compiled as part of the MAREDAT effort. The coccolithophores are a globally occurring group of calcifying phytoplankton of the class Prymnesiophyceae (Jordan et al., 2004).

20 They are thought to play an important role in the global carbon cycle due to their contribution to primary production and export as well as through calcite production (Hay, 2004; Jin et al., 2006), with blooms of up to $100\,000\,\text{km}^2$ observed in some ocean regions (Brown and Yoder, 1994). The coccolithophores have received considerable attention in recent years due to their potential sensitivity to climate change and partic-

25 ularly ocean acidification. The decrease in carbonate saturation state in the oceans caused by rising atmospheric CO_2 is generally expected to have negative effects on calcifying marine organisms due to the increasing energetic cost of calcification (Hofmann et al., 2010). There have, however, been mixed results from experimental and field studies of coccolithophores, with some showing a negative effect of ocean

Coccolithophore biomass distributions

C. J. O'Brien et al.

Title Page

Abstract | Instruments

Data Provenance & Structure

Tables | Figures

|◀ | ▶|

◀ | ▶

Back | Close

Full Screen / Esc

Printer-friendly Version

Interactive Discussion

acidification (e.g Beaufort et al., 2011; Riebesell and Zondervan, 2000) whereas others show no change or even increased calcification and production (Langer et al., 2006; Iglesias-Rodriguez et al., 2008). Changes in ocean temperature, stratification and nutrient supply are also expected to affect coccolithophore distributions, although again the direction of this change is unclear (Hood et al., 2006; Iglesias-Rodríguez, 2002). Given these uncertainties, it is more important than ever to understand the current distribution of coccolithophores in the global oceans.

Remote sensing approaches are frequently used to study the distribution of coccolithophore blooms (e.g. Smyth, 2004; Brown and Yoder, 1994; Iglesias-Rodríguez, 2002; Hirata et al., 2011). The reflective properties of the calcite-based coccoliths allow blooms to be observed in satellite images (Holligan et al., 1983), providing great potential for improving our understanding of coccolithophore distributions on a global scale. There are, however, several limitations to this approach. Firstly, satellite images pick up the optical properties of the calcite-based coccoliths themselves and do not distinguish between living cells and shedded coccoliths (Tyrell and Merico, 2004). Secondly, satellite data are limited to waters within the optical depth of the satellite and provide no information as to the vertical structure of cells within the water column or cells occurring below this depth. Finally, more detailed taxonomic information cannot yet be obtained from satellite images. There is, therefore, a continuing need for in situ observations of coccolithophores in order to better understand their distribution, ecology and contribution to global plankton biomass.

This database compiles existing published and unpublished coccolithophore abundance data and provides standardised biomass estimates using species-specific conversion factors. We also provide a detailed discussion of our conversion methods and quality control procedures and discuss the uncertainties associated with the biomass values. Although this dataset was born from the needs of the modelling community, we anticipate that it will be of use to scientists from a range of fields including biological oceanography, marine ecology, biogeochemistry and remote sensing.

Full Screen / Esc

2 Data

2.1 Origin of data

Our data consists of abundance measurements obtained from several existing databases (NMFS-COPEPOD, BODC, OBIS, OCB DMO, Pangaea, WOD09, OOV)[1], as well as published and unpublished data from a number of contributing authors (P. Ajani, H. Andruleit, J. Arístegui, L. Beaufort, M. Estrada, D. Karentz, E. Kopczyńska, R. Lee, T. Pritchard and C. Widdicombe).

Table 1 summarizes the origin of all datasets, sorted in temporal order. The database contains 58 384 data points when counts of individual taxa are considered separately, which equates to 12 391 samples of total coccolithophore abundance collected from 7049 depth-resolved stations.

2.2 Biomass conversion

To convert the abundance data to biomass estimates, we first estimated cell biovolumes for each of the taxonomic groups reported in the database. Coccolithophore taxonomy has been subject to numerous revisions over the timespan of the dataset, making it challenging to match historical data to current species names and descriptions. For consistency, data entries were matched to currently accepted species names following the taxonomic scheme of Jordan et al. (2004) wherever possible. Where full taxonomic information was not provided, data were matched to the lowest taxonomic group possible. Data that could not be assigned to a particular taxonomic group were

---

[1]NMFS-COPEPOD: National Marine and Fisheries Service – The Coastal & Oceanic Plankton Ecology, Production, & Observation Database; BODC: British Oceanographic Data Centre; OBIS: the Ocean Biogeographic Information System; OCB DMO: Ocean Carbon and Biogeochemistry Coordination and Data Management Office; Pangaea: Data Publisher for Earth and Environmental Science; WOD09: World Ocean Database 2009; OOV: Observatoire Océanologique de Villefrance-sur-Mer.

categorised as unidentified coccolithophores. We identified a total of 196 taxonomic groups for this dataset (see Supplement Table S1), ranging from identifications at the sub-species to the family level. Additionally, some datasets provided combined counts of coccolithophores without further taxonomic information.

For our biomass conversions, we began by converting only cell counts for which full species or sub-species identifications were provided. Each species/sub-species was assigned an idealised shape (e.g. sphere, prolate sphere, cone) based on the work of Hillebrand et al. (1999) and Sun (2003) as well as species descriptions in the literature. We then determined the range of cell dimensions (e.g. diameter, length, width) for each species or sub-species in the database based on a literature survey (see Supplement Table S1). This information was used to calculate cell biovolume estimates (units: μm^3). For some datapoints, cell dimensions were provided alongside cell counts. In these cases the provided measurements were used in preference to our literature-based values.

To account for the uncertainty associated with these estimates, we calculated three estimates of cell biovolume based on the minimum, maximum and mid-point of reported cell dimensions. Biovolume estimates were then further converted to carbon biomass (units: $\mu g\,C\,l^{-1}$) using the prymnesiophyte-specific conversion factor developed by Menden-Deuer and Lessard (2000). Biovolume and biomass values based on the mid-point are hereafter referred to as "mean" biovolume and biomass.

For 23 species only a single set of dimensions or a single biovolume value was reported in the literature. In these cases, we have assumed the reported values to be the mean estimates. Minimum and maximum biovolume values were estimated for these species based on the ratios of minimum and maximum biovolume to mean biovolume observed for all other species in the database. These ratios were found to be 0.5 (± standard deviation of 0.2) for minimum biovolume/mean biovolume, and 2.1 (±0.8) for maximum biovolume/mean biovolume.

For cell counts with identifications only to the level of genus or family, or for combined counts of multiple species, we calculate minimum and maximum biomass values per

cell based on the absolute minimum and maximum of all species reported for that taxonomic group. Mean biomass values per cell were calculated by taking the mean of all reported biomass values for species within the taxonomic group. Taking the mean of the biomass values avoided weighting mean biomass values towards a single large species. For some genera, however, insufficient species-level data were available to calculate biomass using this approach. In these cases we were able to obtain a range of cell dimensions from the literature, and calculated biovolumes and biomasses using the mid-point of these values as detailed above for the species-specific cell counts.

For cell counts of unidentified coccolithophores, we have chosen to use a spherical cell with diameter of 10 µm to calculate our mean biovolume and biomass estimates. This value was selected based on the diameters of species most commonly occurring in the database. The large uncertainty associated with this value is taken into account by providing minimum and maximum biovolume and biomass estimates based on the absolute minimum and maximum values across all species in the database.

Following the biomass conversions, data were compiled to total coccolithophore biomass per sample for the purposes of further analyses. Further taxonomic information is reported in the attached dataset (http://doi.pangaea.de/10.1594/PANGAEA.785092) and coccolithophore biodiversity patterns will be discussed in O'Brien et al. (2012).

2.3 Quality control

Our quality control procedure flagged data based on a number of criteria, with flag values (1–4) provided in the data table. Flag 1 was applied to 33 samples that included observations of the species *Thoracosphaera heimii* – this species was originally thought to be a coccolithophore, but further investigations have shown it to be a calcified dinoflagellate cyst (Tangen et al., 1982). Flag 2 was applied to 205 samples for which only biomass values were provided, without corresponding cell counts; and flag 3 is applied to 482 samples with integrated water column values rather than discrete depth

measurements, or to samples for which no depth information was provided. Flag 4 was assigned to outliers identified by the statistical analyses to be outlined below.

For the next stage of the quality control process, we removed samples with flags 2 and 3 and corrected samples with flag 1 to remove counts of *T. heimii*. For the remaining 9194 non-zero samples, we used Chauvenet's criterion to identify statistical outliers in the log-normalized biomass data (Buitenhuis et al., 2012; Glover et al., 2011). Based on this analysis, we identified one sample with a biomass value with probability of deviation from the mean greater than $1/2n$, with $n = 9194$ being the number of non-zero samples (two-sided z-score: $|zc| = 4.05$). This sample is denoted by a flag value of 4.

Based on our full quality control procedure we removed a total of 689 flagged samples for the purposes of our analyses, and a further 32 samples were corrected to remove the contribution of *T. heimii* to total coccolithophore biomass (note: one sample contained data for *T. heimii* only). All flagged data are included in the published dataset in the event that a user has different requirements for the quality control procedure.

3 Results

Excluding flagged data, the database contains coccolithophore biomass observations for 11 702 samples, collected from 6766 depth-resolved stations (Fig. 1). 2509, or 21.4 % of samples, were found to be zero values. These data were retained in the dataset, since confirmed zero values hold valuable information for the study of plankton distributions. There is, however, inconsistency in the reporting of zero values in plankton datasets: often abundance data are reported only for a limited range of target groups that are expected to be present. There is also likely to be a bias due to sampling focusing on areas where coccolithophores are expected to occur. Values reported in the subsequent sections are therefore calculated based on non-zero data only. Where zero-datapoints are included, this value follows in parentheses. Arithmetic mean values are reported plus or minus one standard deviation. We also provide median biomass

values, as these are less influenced by high values and provide a better representation of the central tendency of the data.

3.1 Spatial and temporal coverage

The database includes non-zero coccolithophore observations from the surface to a depth of 500 m (Fig. 2b, with 83.9 % of observations (84.1 % with zero values included) from the upper 50 m and 61.5 % (63.3 %) from the upper 10 m of the water column. Mean depth is 27.0 (±40.5) m and median depth is 10.0 m.

Data are reported from all ocean basins, with 54.4 % of samples (58.9 % with zero values included) from the Northern Hemisphere and 45.4 % (40.9 %) from the Southern Hemisphere (Table 3). 31.6 % of non-zero data are from the Atlantic Ocean, 40.2 % from the Pacific Ocean and 10.4 % from the Indian Ocean. Despite the high number of observations reported from the Pacific compared to the Atlantic, the spatial coverage of this ocean basin is relatively poor, with many observations limited to intensively studied regions in Peruvian and Japanese coastal waters.

9.9 % of non-zero observations are from the polar regions, with 5.1 % from the Southern Ocean and 4.8 % from Arctic waters. Coccolithophores are reported to be present in only one sample below 60° S (Table 2). In contrast, the database contains non-zero observations of coccolithophores in Arctic waters up to a maximum of 88.92° N. 46.3 % of data are from tropical waters between 20° S and 20° N.

Data are reported from the years 1929 to 2008 (Figs. 2, 3). A total of 66 non-zero observations are reported for 1929–1930, with no further observations until 1954. 78.7 % of observations were collected between 1980 and 2008, and 51.8 % between 1990 and 2008. Data are reported from all months of the year in both hemispheres, although relatively few data were collected during the winter months (13.6 % of all NH data, 15.6 % of SH data, Table 3). Northern Hemisphere data are strongly biased towards summer observations (38.4 % of all data).

3.2 Biomass distribution

3.2.1 Geographical distribution

Coccolithophore biomass values range from 7.7×10^{-5} to $501.7\,\mu g\,Cl^{-1}$. The global mean is $3.8\,\mu g\,Cl^{-1} \pm 21.0\,\mu g\,Cl^{-1}$ and median biomass is $0.25\,\mu g\,Cl^{-1}$. Highest biomass values were recorded in the Northern Hemisphere between 60 and 70° N (Fig. 6, Table 2), with a mean biomass of $14.0 \pm 57.8\,\mu g\,Cl^{-1}$, median of $0.40\,\mu g\,Cl^{-1}$ and maximum of $501.7\,\mu g\,Cl^{-1}$. There is a sharp drop in biomass values north of 70° N.

In the Southern Hemisphere, the highest biomass value reported is $178.3\,\mu g\,Cl^{-1}$ in the Eastern Indian Ocean (19.39° S and 110.5° E). Biomass values are highest around 20° S and decline toward the equator, where the highest biomass reported is $1.6\,\mu g\,Cl^{-1}$. Biomass values fall rapidly below 50° S.

Strong differences can be observed between the Atlantic and Pacific Ocean, with Atlantic biomass values reaching $501.7\,\mu g\,Cl^{-1}$ (mean 7.80 ± 31.59, median $0.48\,\mu g\,Cl^{-1}$) compared to just $79.44\,\mu g\,Cl^{-1}$ in the Pacific (mean 1.05 ± 3.63, median $0.17\,\mu g\,Cl^{-1}$). The relatively poor spatio-temporal coverage of Pacific Ocean observations, however, may contribute to this discrepancy. Indian Ocean biomass values reach a maximum of $178.31\,\mu g\,Cl^{-1}$, with a mean of 4.46 ± 13.31 and median of $0.13\,\mu g\,Cl^{-1}$.

In the Southern Ocean, the maximum biomass value reported is $0.81\,\mu g\,Cl^{-1}$, mean biomass is $0.088 \pm 0.11\,\mu g\,Cl^{-1}$ and median biomass is $0.049\,\mu g\,Cl^{-1}$. Arctic biomass values are much lower, with a maximum of $0.063\,\mu g\,Cl^{-1}$, mean of $0.013 \pm 0.016\,\mu g\,Cl^{-1}$ and median of $0.0052\,\mu g\,Cl^{-1}$.

3.2.2 Depth distribution

Highest biomass values are reported in surface waters and decline with depth (Figs. 2b, 4), although biomass values of up to $93.3\,\mu g\,Cl^{-1}$ are still reported at 100 m depth. Mean biomass for the surface layer (0–10 m) is $3.6 \pm 20.4\,\mu g\,Cl^{-1}$ and median biomass is $0.36\,\mu g\,Cl^{-1}$. Biomass values below 200 m reach a maximum of $1.2\,\mu g\,Cl^{-1}$. The

deepest observations of coccolithophores are at 500 m depth, with biomasses reaching a maximum of just $0.6\,\mu g\,C\,l^{-1}$.

3.2.3 Seasonal distribution

The data show a clear seasonal cycle in the Northern Hemisphere, with biomass values reaching just $2.3\,\mu g\,C\,l^{-1}$ in December and a maximum of up to $500\,\mu g\,C\,l^{-1}$ in the summer months (June–July, Fig. 7). In the Southern Hemisphere the seasonal cycle is less evident, possibly due to the greater contribution of data from low latitudes where seasonal changes are less pronounced.

3.2.4 Uncertainty

The uncertainty associated with our conversions of cell abundance to carbon biomass is depicted in Fig. 5. Biomass estimates are best constrained where detailed taxonomic information is available, and for samples containing species for which a limited range of cell sizes has been reported. Very high uncertainty (range of biomass values greater than 7000 % of the mean biomass) is associated with counts of unidentified coccolithophores. This is to be expected given the extremely broad range of cell sizes reported for the approximately 200 known coccolithophore species (see Supplement Table S1).

4 Discussion

There are many sources of uncertainty associated with our calculations. We have attempted to quantify the uncertainty associated with variable cell dimensions by providing minimum and maximum biomass values for each datapoint, but this does not represent the full range of uncertainty associated with our biomass values. Few observations of cell dimensions are reported in the literature for most species, and the number of cells that have been studied to derive the given ranges is rarely reported.

Measurements are often from a single geographical location, meaning that cell size variation between strains is not accounted for. There is additionally inconsistency as to whether the range of cell sizes reported is the full range of cell sizes that occurs or only those most commonly observed. A further source of uncertainty is the generalisation of at times complex cell geometry to fit a particular geometric form.

Some datasets report biomass values in addition to abundance data. While we have chosen to use our own conversion methods for consistency, it is likely that the original biomass values are based on more accurate estimates of cell size. All original biomass values are included in the submitted database and can be substituted for our estimates if desired.

Furthermore, our biomass estimates do not distinguish between organic and inorganic carbon, since reported cell dimensions generally refer to the total dimensions including coccoliths. This adds additional uncertainty to our biomass estimates, since the conversion factor we use has been developed for estimating the organic carbon biomass of non-calcifying cells. The ratio of inorganic : organic carbon has been shown to vary considerably with environmental conditions (Zondervan, 2007), with ratios for the species *Emiliania huxleyi* alone ranging from 0.51 to 1.66 (Paasche, 2002).

Users of the gridded datafile should take into consideration the sparse nature of the original data. Often monthly mean gridded values have been derived from relatively few individual datapoints that do not represent the full range of values that occur in a given location. We expect to see a bias toward higher biomass values, given that studies are often conducted in locations and times of year when blooms are expected to occur.

5 Conclusions

This database represents the largest effort to date to compile coccolithophore abundance observations and provide standardised biomass estimates to the scientific community. We report our biovolume and biomass conversion procedures in detail and discuss the associated uncertainties.

We anticipate that this dataset, together with others from the MAREDAT special issue, will be a valuable resource for studies of plankton distributions and ecology and in particular for the evaluation and development of marine ecosystem models. While data are clearly lacking for certain regions, the dataset nevertheless represents the largest available compilation of global coccolithophore abundance and biomass. We hope to improve the spatial and temporal coverage of the dataset as additional data become available in the future.

Appendix A

A1   Data table

A full data table containing all biomass data points can be downloaded from the data archive PANGAEA (http://doi.pangaea.de/10.1594/PANGAEA.785092). The data file contains longitude, latitude, depth, sampling time, abundance counts and biomass concentrations, as well as the full data references.

A2   Gridded netcdf biomass product

Monthly mean biomass data have been gridded onto a $360 \times 180°$ grid, with a vertical resolution of 33 depth levels (equivalent to World Ocean Atlas depths) and a temporal resolution of 12 months (climatological monthly means). This dataset is provided in netcdf format for easy use in model evaluation exercises. The netcdf file can be downloaded from PANGAEA (http://doi.pangaea.de/10.1594/PANGAEA.785092). This file contains total and non-zero abundance and biomass values. For all fields, the means, medians and standard deviations resulting from multiple observations in each of the $1°$ pixels are given. The ranges in biomass values due to uncertainties in cell size are not included as variables in the netcdf product, but are given as ranges (minimum cell biomass, maximum cell biomass) in the data table.

References

Ajani, P., Lee, R., Pritchard, T., and Krogh, M.: Phytoplankton dynamics at a long-term coastal station off Sydney, Australia, J. Coastal Res., 34, 60–73, 2001. 511

Anderson, T. R.: Plankton functional type modelling: running before we can walk?, J. Plankton Res., 27, 1073–1081, doi:10.1093/plankt/fbi076, 2005. 494

Andruleit, H., Stäger, S., Rogalla, U., and Cepek, P.: Living coccolithophores in the northern Arabian Sea: ecological tolerances and environmental control, Mar. Micropaleontol., Supplement, 49, 157–181, doi:10.1016/S0377-8398(03)00049-5, 2003. 511

Andruleit, H.: Living coccolithophores recorded during the onset of upwelling conditions off Oman in the western Arabian Sea, J. Nannoplankton Res., 27, 1–14, 2005. 511

Andruleit, H.: Status of the Java upwelling area (Indian Ocean) during the oligotrophic Northern Hemisphere winter monsoon season as revealed by coccolithophores, Mar. Micropaleontol., 64, 36–51, doi:10.1016/j.marmicro.2007.02.001, 2007. 511

Assmy, P.: Phytoplankton abundance measured on water bottle samples at stations PS65/424-3, 514-2, 570-4 & 587-1, Alfred Wegener Institute for Polar and Marine

Research, Bremerhaven, doi:10.1594/PANGAEA.603388, doi:10.1594/PANGAEA.603393, doi:10.1594/PANGAEA.603398 and doi:10.1594/PANGAEA.603400, 2007. 511

Beaufort, L., Probert, I., de Garidel-Thoron, T., Bendif, E. M., Ruiz-Pino, D., Metzl, N., Goyet, C., Buchet, N., Coupel, P., Grelaud, M., Rost, B., Rickaby, R. E. M., and de Vargas, C.: Sensitivity of coccolithophores to carbonate chemistry and ocean acidification, Nature, 476, 80–83, doi:10.1038/nature10295, 2011. 495

Brown, C. and Yoder, J.: Coccolithophorid blooms in the global ocean, J. Geophys. Res., 99, 7467–7482, 1994. 494, 495

Buitenhuis, E. T., Vogt, M., Bednarsek, N., Doney, S., Leblanc, K., Le Quéré, C., Luo, Y., Moriarty, R., O'Brien, C., O'Brien, T., Peloquin, J., and Schiebel, R.: MAREDAT: Towards a world ocean atlas of MARine Ecosystem DATa, Earth Syst. Sci. Data Discuss., in preparation, 2012.

Dutkiewicz, S., Ward, B. A., Monteiro, F., and Follows, M. J.: Interconnection of nitrogen fixers and iron in the Pacific Ocean: theory and numerical simulations, Global Biogeochem. Cy., 26, 1–16, doi:10.1029/2011GB004039, 2012. 494

Estrada, M.: Phytoplankton assemblages across a NW Mediterranean front: changes from winter mixing to spring stratification, Oecologia Aquatica, 10, 157–185, 1991. 511

Estrada, M. and Delgado, M.: Summer phytoplankton distributions in the Weddell Sea, Polar Biol., 10, 441–449, 1990. 511

Fryxell, G.: Abundance and carbon biomass of phytoplankton at station TT0X_X-CTDX, doi:10.1594/PANGAEA.122734–PANGAEA.122756, 2003. 511

Glover, D. M., Jenkins, W. J., and Doney, S. C.: Modeling Methods for Marine Science, Cambridge University Press, 2011. 499

Grados, C., Flores, G., Villanueva, P., Chang, F., and Ayón, P.: Phytoplankton abundance at stations off Paita in August 1995, Piura, Peru, Instituto del Mar del Peru, doi:10.1594/PANGAEA.603265 and doi:10.1594/PANGAEA.603267, 2007. 511

Hay, W. W.: Carbonate fluxes and calcareous nannoplankton, in: Coccolithophores: from Molecular Processes to Global Impact, edited by: Thierstein, H. and Young, J., Springer, 509–528, 2004. 494

Hillebrand, H., Dürselen, C., Kirschtel, D., Pollingher, U., and Zohary, T.: Biovolume calculation for pelagic and benthic microalgae, J. Phycol., 424, 403–424, 1999. 497

Hirata, T., Hardman-Mountford, N. J., Brewin, R. J. W., Aiken, J., Barlow, R., Suzuki, K., Isada, T., Howell, E., Hashioka, T., Noguchi-Aita, M., and Yamanaka, Y.: Synoptic

Title Page

Abstract | Instruments

Data Provenance & Structure

Tables | Figures

◄◄ | ►►

◄ | ►

Back | Close

Full Screen / Esc

Printer-friendly Version

Interactive Discussion

relationships between surface Chlorophyll-*a* and diagnostic pigments specific to phytoplankton functional types, Biogeosciences, 8, 311–327, doi:10.5194/bg-8-311-2011, 2011. 495

Hofmann, G. E., Barry, J. P., Edmunds, P. J., Gates, R. D., Hutchins, D. A., Klinger, T., and Sewell, M. A.: The effect of Ocean acidification on calcifying organisms in marine ecosystems: an organism-to-ecosystem perspective, Annu. Rev. Ecol. Evol. S., 41, 127–147, doi:10.1146/annurev.ecolsys.110308.120227, 2010. 494

Holligan, P., Viollier, M., Harbour, D., Camus, P., and Champagne-Philippe, M.: Satellite and ship studies of coccolithophore production along a continental shelf edge, Nature, 304, 339–342, 1983. 495

Hood, R., Laws, E., Armstrong, R., Bates, N., Brown, C., Carlson, C., Chai, F., Doney, S., Falkowski, P., and Feely, R.: Pelagic functional group modeling: progress, challenges and prospects, Deep-Sea Res. Pt. II, 53, 459–512, doi:10.1016/j.dsr2.2006.01.025, 2006. 494, 495

Iglesias-Rodríguez, M. D.: Representing key phytoplankton functional groups in ocean carbon cycle models: coccolithophorids, Global Biogeochem. Cy., 16, 1–20, doi:10.1029/2001GB001454, 2002. 494, 495

Iglesias-Rodriguez, M. D., Halloran, P. R., Rickaby, R. E. M., Hall, I. R., Colmenero-Hidalgo, E., Gittins, J. R., Green, D. R. H., Tyrrell, T., Gibbs, S. J., von Dassow, P., Rehm, E., Armbrust, E. V., and Boessenkool, K. P.: Phytoplankton calcification in a high-CO_2 world., Science, 320, 336–40, doi:10.1126/science.1154122, 2008. 495

Jin, X., Gruber, N., Dunne, J. P., Sarmiento, J. L., and Armstrong, R. A.: Diagnosing the contribution of phytoplankton functional groups to the production and export of particulate organic carbon, $CaCO_3$, and opal from global nutrient and alkalinity distributions, Global Biogeochem. Cy., 20, 1–17, 2006. 494

Jordan, R., Cros, L., and Young, J.: A revised classification scheme for living haptophytes, Micropaleontology, 50, 55–79, 2004. 494, 496

Kopczynska, E. E., Savoye, N., Dehairs, F., Cardinal, D., and Elskens, M.: Spring phytoplankton assemblages in the Southern Ocean between Australia and Antarctica, Polar Biol., 31, 77–88, doi:10.1007/s00300-007-0335-6, 2007. 511

Langer, G., Geisen, M., Baumann, K.-H., Kläs, J., Riebesell, U., Thoms, S., and Young, J. R.: Species-specific responses of calcifying algae to changing seawater carbonate chemistry, Geochem. Geophy. Geosy., 7, Q09006, doi:10.1029/2005GC001227, 2006. 495

Le Quéré, C., Harrison, S., Prentice, I., Buitenhuis, E., Aumont, O., Bopp, L., Claustre, H., Da Cunha, L., Geider, R., Giraud, X., Klaas, C., Kohfeld, K., Legendre, L., Manizza, M., Platt, T., Rivkin, R., Sathyendranath, S., Uitz, J., Watson, J., and Wolf-Gladrow, D.: Ecosystem dynamics based on plankton functional types for global ocean biogeochemistry models, Glob. Change Biol., 11, 2016–2040, doi:10.1111/j.1365-2486.2005.1004.x, 2005. 494

Manizza, M., Buitenhuis, E. T., and Le Quéré, C.: Sensitivity of global ocean biogeochemical dynamics to ecosystem structure in a future climate, Geophys. Res. Lett., 37, 3–7, doi:10.1029/2010GL043360, 2010. 494

Marinov, I., Doney, S. C., and Lima, I. D.: Response of ocean phytoplankton community structure to climate change over the 21st century: partitioning the effects of nutrients, temperature and light, Biogeosciences, 7, 3941–3959, doi:10.5194/bg-7-3941-2010, 2010. 494

Marshall, H. G.: Phytoplankton distribution off the North Carolina coast, Am. Midl. Nat., 82, 241–257, doi:10.2307/2423833, 1969. 511

Menden-Deuer, S. and Lessard, E. J.: Carbon to volume relationships for dinoflagellates, diatoms, and other protist plankton, Limnol. Oceanogr., 45, 569–579, 2000. 497

Mohan, R., Mergulhao, L. P., Guptha, M., Rajakumar, A., Thamban, M., AnilKumar, N., Sudhakar, M., and Ravindra, R.: Ecology of coccolithophores in the Indian sector of the Southern Ocean, Mar. Micropaleontol., 67, 30–45, doi:10.1016/j.marmicro.2007.08.005, 2008. 511

O'Brien, C. J.: In preparation, 2012.

Omex I project members and Wassmann, P.: Phytoplankton abundance measured on water bottle samples at station JMX_XX, doi:10.1594/PANGAEA.202662–PANGAEA.202700, 2004. 511

Paasche, E.: A review of the coccolithophorid *Emiliania huxleyi* (Prymnesiophyceae), with particular reference to growth, coccolith formation, and calcification-photosynthesis interactions, Phycologia, 40, 503–529, 2002. 503

Pagou, K. and Assimakopoulou, G.: Abundance of microplankton from bottles SEPT-1999-K1– APRIL-2000-K6, Hellenic Center of Marine Research, Institut of Oceanography, Greece, doi:10.1594/PANGAEA.687204–PANGAEA.687209 and doi:10.1594/PANGAEA.688625– PANGAEA.688633, 2008. 511

Ramos, E.: Phytoplankton abundance in surface water in 1992, Ancon, Peru, Universidad Nacional Mayor de San Marcos, doi:10.1594/PANGAEA.465179 to doi:10.1594/PANGAEA.465192, 2006. 511

Coccolithophore biomass distributions

C. J. O'Brien et al.

Title Page

| Abstract | Instruments |

Data Provenance & Structure

| Tables | Figures |

|◀ | ▶|

| ◀ | ▶ |

| Back | Close |

Full Screen / Esc

Printer-friendly Version

Interactive Discussion

Ratkova, T.: ArcOD – Phytoplankton from the White Sea, Barents Sea, Norwegian Sea and Arctic Basin 1993–2003, Ocean Biogeographic Information System, unpublished data, 2012. 511

Riebesell, U. and Zondervan, I.: Reduced calcification of marine plankton in response to increased atmospheric CO_2, Nature, 407, 364–367, 2000. 495

Schiebel, R.: Distribution of diatoms, coccolithophores and planktic foraminifers along a trophic gradient during SW monsoon in the Arabian Sea, Mar. Micropaleontol., 51, 345–371, doi:10.1016/j.marmicro.2004.02.001, 2004a. 511

Schiebel, R.: Distribution of diatoms, coccolithophores and planktic foraminifera in the Arabian Sea, doi:10.1594/PANGAEA.736805, 2004b. 511

Silver, M.: Vertigo KM0414 phytoplankton species data and biomass data: abundance and fluxes from CTDs, Ocean Carbon and Biogeochemistry Data System, OCB DMO, WHOI, 2009. 511

Smyth, T. J.: Time series of coccolithophore activity in the Barents Sea, from twenty years of satellite imagery, Geophys. Res. Lett., 31, 2–5, doi:10.1029/2004GL019735, 2004. 495

Sun, J.: Geometric models for calculating cell biovolume and surface area for phytoplankton, J. Plankton Res., 25, 1331–1346, doi:10.1093/plankt/fbg096, 2003. 497

Takahashi, K. and Okada, H.: Environmental control on the biogeography of modern coccolithophores in the Southeastern Indian Ocean offshore of Western Australia, Mar. Micropaleontol., 39, 73–86, 2000. 511

Tangen, K., Brand, L. E., Blackwelder, P. L., and Guillard, R. R. L.: *Thoracosphaera heimii* (Lohmann) Kamptner is a dinophyte: observations on its morphology and life cycle, Mar. Micropaleontol., 7, 193–212, 1982. 498

Tyrell, T. and Merico, A.: *Emiliania huxleyi*: bloom observations and the conditions that induce them, in: Coccolithophores: from Molecular Processes to Global Impact, edited by: Thierstein, H. R. and Young, J., Springer, 75–97, 2004. 495

Vogt, M., Vallina, S. M., Buitenhuis, E. T., Bopp, L., and Le Quéré, C.: Simulating dimethylsulphide seasonality with the dynamic green ocean model PlankTOM5, J. Geophys. Res., 115, 1–21, doi:10.1029/2009JC005529, 2010. 494

Widdicombe, C. E., Eloire, D., Harbour, D., Harris, R. P., and Somerfield, P. J.: Long-term phytoplankton community dynamics in the Western English Channel, J. Plankton Res., 32, 643–655, doi:10.1093/plankt/fbp127, 2010. 511

Title Page

Abstract | Instruments

Data Provenance & Structure

Tables | Figures

|◄ | ►|

◄ | ►

Back | Close

Full Screen / Esc

Printer-friendly Version

Interactive Discussion

Zeitzschel, B., Deckers, M., Karrasch, B., Kremling, K., Podewski, S., Stienen, C., and Ullrich, S.: Hydrochemistry and biological data measured on water bottle samples during METEOR cruise M10/2, doi:10.1594/PANGAEA.66713, 2002. 511

Zondervan, I.: The effects of light, macronutrients, trace metals and CO_2 on the production of calcium carbonate and organic carbon in coccolithophores: a review, Deep-Sea Res. Pt. II, 54, 521–537, doi:10.1016/j.dsr2.2006.12.004, 2007. 503

Title Page

Abstract | Instruments

Data Provenance & Structure

Tables | Figures

|◄ | ►|

◄ | ►

Back | Close

Full Screen / Esc

Printer-friendly Version

Interactive Discussion

Table 1. List of data contributions, sorted in temporal order.

Investigator/Institute	Year(s)	Region	Data points	Flagged	Reference
Meteor	1929–1930	N Atlantic	66	–	NMFS-COPEPOD
Murmansk Marine Biological Institute, Russia	1954–1973	Barents Sea	267	–	WOD09
H. Marshall	1965	NW Sargasso Sea	32	32	Marshall (1969)
ORSTOM	1965	Tropical Pacific	161	–	WOD09
Instituto del Mar del Peru	1966–2005	Peruvian coastal zone	2668	92	WOD09
NOAA/University of Alaska (OCSEAP)	1969–1978	Gulf of Alaska	293	265	WOD09
J. Throndsen	1970	Tropical Pacific/Caribbean	105	–	NMFS-COPEPOD
SAHFOS	1970–1999	N Atlantic	391	–	WOD09
Institute of Biology of the Southern Seas, Ukraine	1972–1990	Indian Ocean	558	–	NMFS-COPEPOD
Tokyo University Ocean Research Institute, Japan	1975	W Pacific	68	–	WOD09
National Institute for Environmental Studies, Japan	1976–1985	W Pacific	120	44	WOD09
NOAA	1976–1977	Puget Sound, WA, US	18	–	WOD09
Japan Meteorological Agency	1977–1986	W Pacific	1963	29	WOD09
Institute of Ocean Sciences, Sidney, Canada	1979	US Coast (Oregon)	29	–	WOD09
E. Baldina et al.	1979–1986	Tropical Atlantic	941	–	NMFS-COPEPOD
Aomori Prefectural Fisheries Experimental Station, Japan	1980	West Pacific	2	–	WOD09
TPFS	1983	West Pacific	1	–	WOD09
AtlantNIRO	1984–1991	Atlantic	365	–	NMFS-COPEPOD
M. Estrada	1985	Mediterranean Sea	260	–	Estrada (1991), Estrada (unpublished data)
M. Estrada	1985	Weddell Sea	126	–	Estrada and Delgado (1990), Estrada (unpublished data)
Osaka Prefectural Fisheries Experimental Station, Japan	1985	W Pacific	8	8	WOD09
P. Tett	1988–1989	North Sea	50	–	BODC
D. Harbour	1989	North Atlantic	33	–	BODC
B. Zeitzschel	1989	North Atlantic	205	205	Zeitzschel et al. (2002)
D. Harbour	1990	North Atlantic	68	–	BODC
D. Harbour	1991	North Atlantic	78	–	BODC
AESOPS	1992	Southern Ocean	31	–	WOD09
G. Fryxell	1992	Equatorial Pacific	186	–	Fryxell (2003)
K. Takahashi and H. Okada	1992	SE Indian Ocean	114	–	Takahashi and Okada (2000)
M. Fiala	1992–1995	Southern Ocean	73	–	OOV
E. Ramos	1992–2005	Peruvian Coastal Zone	229	–	Ramos (2006)
C. Widdicombe	1992–2008	English Channel	625	–	Widdicombe et al. (2010)
H. Andruleit	1993	Arabian Sea	71	–	Andruleit (2003)
R. Uncles	1993–1995	North Sea	20	–	BODC
P. Wassman and T. Ratkova	1993–2003	Arctic/Sub-Arctic	108	–	Ratkova(2012)
D. Harbour	1994	Arabian Sea	65	–	BODC
OMEX I project members; P. Wassman	1994	NE Atlantic	186	–	Omex I project members and Wassmann (2004)
C. Grados	1995	Peruvian Coastal Zone	12	–	Grados et al. (2007)
R. Schiebel	1995–1997	Arabian Sea	49	–	Schiebel (2004a,b)
J. Aiken, T. Bale, P. Holligan, A. Poulton and D. Robins	1995–2000	Atlantic	408	–	BODC
G. Tarran	1996	North Atlantic	199	–	BODC
P. Ajani, R. Lee and T. Pritchard	1997–1998	SE Australia	45	45	Ajani et al. (2001)
H. Andruleit	1999	E Indian Ocean	45	–	Andruleit (2007)
K. Pagou and G. Assimakopoulou	1999–2000	Aegean Sea	52	–	Pagou and Assimakopoulou (2008)
H. Andruleit	2000	Arabian Sea	22	–	Andruleit (2005)
D. Karentz	2000	E Pacific	7	–	Karentz (unpublished data)
E. Kopczyńska	2001	Southern Ocean	13	–	Kopczyńska et al. (2007)
H. Andruleit	2001–2002	E Pacific	49	–	Andruleit (unpublished data)
J. Arístegui	2003–2004	N Atlantic	152	–	Arístegui (unpublished data)
P. Assmy	2004	Southern Ocean	28	–	Assmy (2007)
L. Beaufort	2004	Pacific	99	–	Beaufort (unpublished data)
R. Mohan	2004	Southern Ocean	131	–	Mohan et al. (2008)
M. Silver	2004	Hawaii	13	–	Silver (2009)

Table 2. Seasonal distribution of abundance data for the Northern and Southern Hemisphere. Number of data points for each month. All: all data, non-zero: data with non-zero carbon biomass.

Month	Globe all	Globe non-zero	NH all	NH non-zero	SH all	SH non-zero
Jan	737	367	489	177	247	189
Feb	1271	922	389	260	881	662
Mar	872	729	489	367	383	362
Apr	942	793	433	317	500	467
May	1095	935	634	534	461	401
Jun	1095	757	845	544	246	213
Jul	1251	906	1104	781	146	125
Aug	1053	942	697	607	356	335
Sep	1111	1005	810	728	290	266
Oct	1304	975	699	441	605	534
Nov	752	671	245	196	507	475
Dec	219	191	59	50	160	141
Spring	–	–	1556	1218	1402	1275
Summer	–	–	2646	1932	1288	992
Autumn	–	–	1754	1365	1344	1230
Winter	–	–	937	487	748	673
Total	11 702	9193	6893	5002	4782	4170

Table 3. Latitudinal distribution of quality-controlled data in ten degree latitudinal bands (−90° to 90°). All data: total number of data points; non-zero data: number of non-zero biomass values; mean, standard deviation, median and maximum biomass values calculated from non-zero data only.

Latitudinal band	All data	Non-zero data	Mean	S.D.	Median	Max
−90−−80°	0	0	–	–	–	–
−80−−70°	60	0	–	–	–	–
−70−−60°	66	1	0.0074	–	0.0074	0.0074
−60−−50°	480	456	0.26	0.83	0.054	8.6
−50−−40°	116	77	6.7	9.4	2.7	48.7
−40−−30°	231	207	3.3	9.6	0.56	89.0
−30−−20°	256	247	7.6	15.9	0.42	114.6
−20−−10°	1754	1467	2.6	8.8	0.37	178.3
−10−0°	1819	1715	0.83	2.6	0.21	73.0
0–10°	1055	860	0.33	0.69	0.13	9.0
10–20°	502	315	0.85	1.5	0.36	16.6
20–30°	759	420	0.37	0.68	0.083	5.5
30–40°	1340	773	0.17	0.38	0.042	3.8
40–50°	820	521	1.5	3.2	0.40	45.7
50–60°	1747	1500	12.3	34.3	1.3	418.5
60–70°	451	451	14.0	57.8	0.40	501.7
70–80°	209	146	0.36	0.49	0.20	3.0
80–90°	37	37	0.094	0.20	0.029	1.1
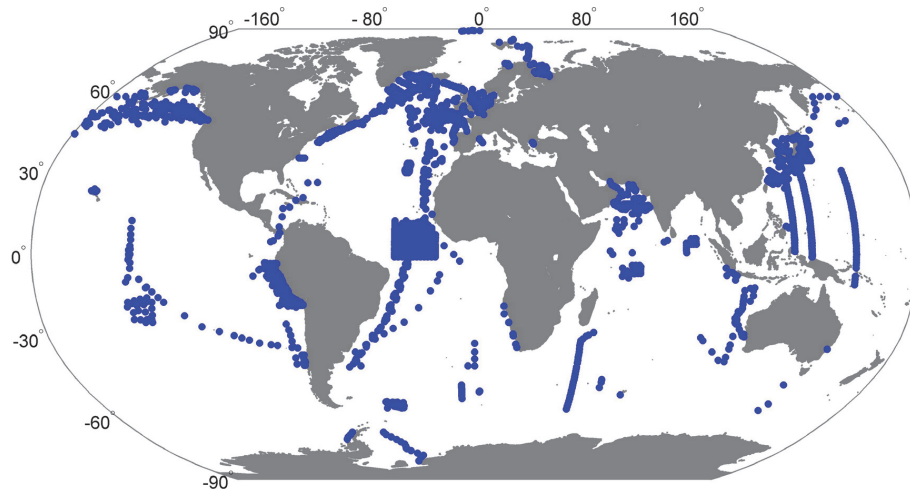
Fig. 1. Global distribution of coccolithophore observations included in the dataset.
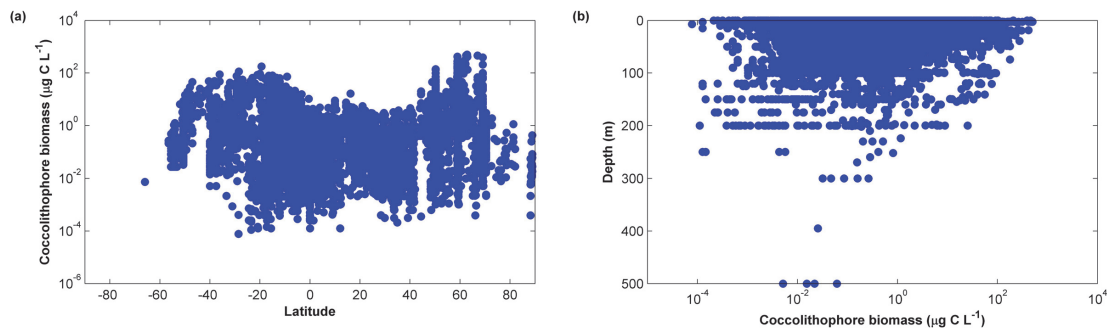
Fig. 2. Distribution of coccolithophore biomass ($\mu g\,C\,l^{-1}$) **(a)** as a function of latitude and **(b)** as a function of depth.
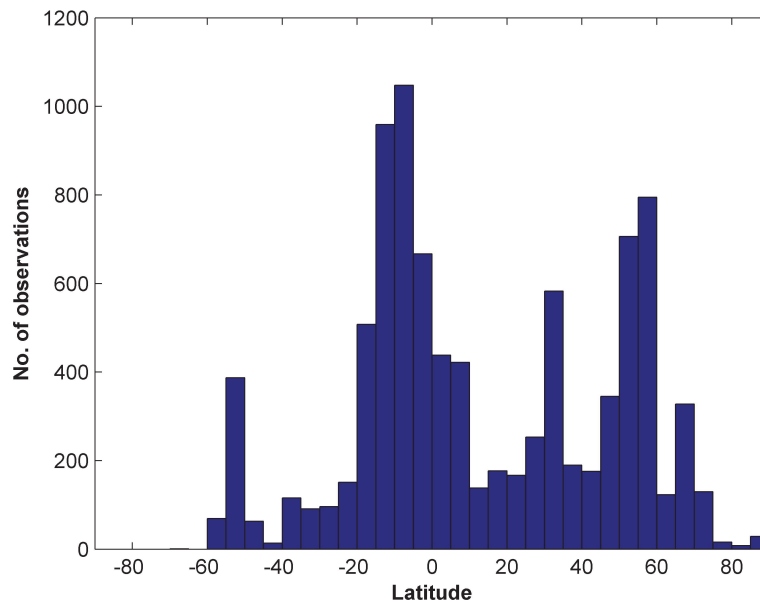
Fig. 3. Frequency distribution of coccolithophore observations as a function of latitude for the period 1929–2008.

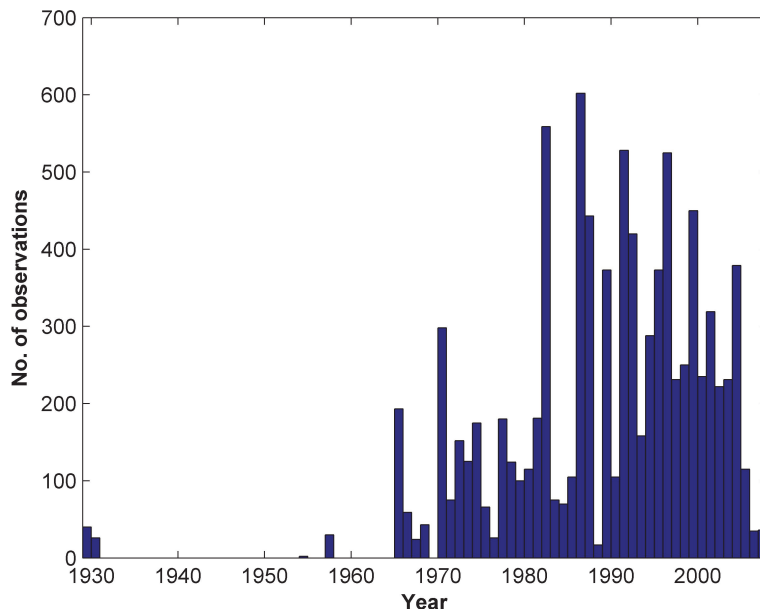**Fig. 4.** Frequency distribution of coccolithophore observations by year, for the period 1929–2008.
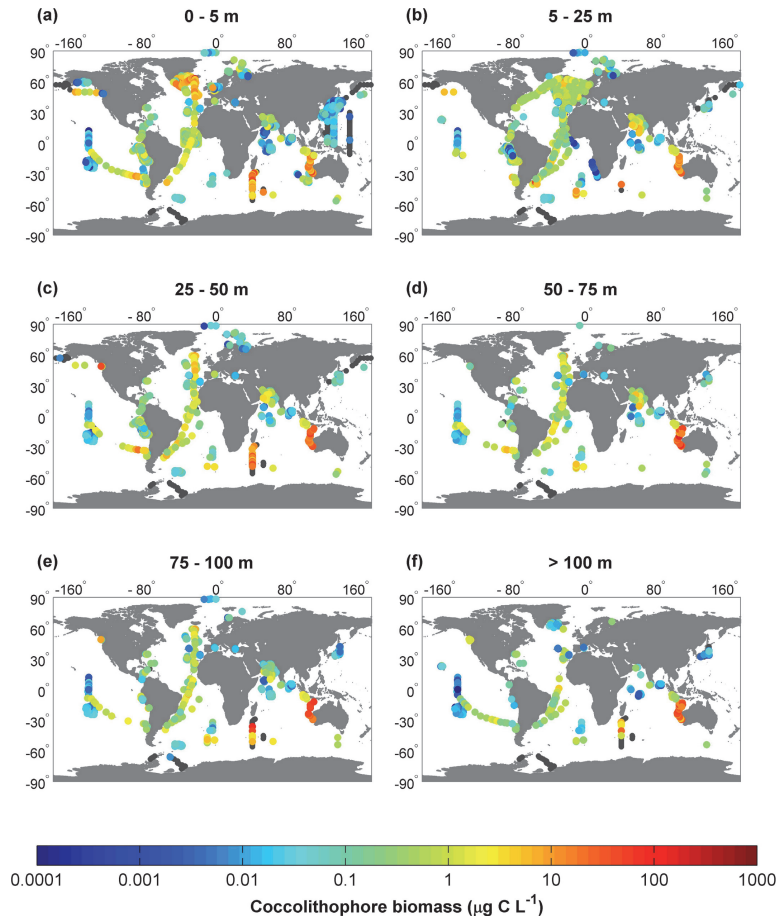
Fig. 5. Mean coccolithophore carbon biomass (μg C l^{-1}) for six depth bands **(a)** 0–5 m **(b)** 5–25 m **(c)** 25–50 m **(d)** 50–75 m **(e)** 75–100 m and **(f)** > 100 m depth.
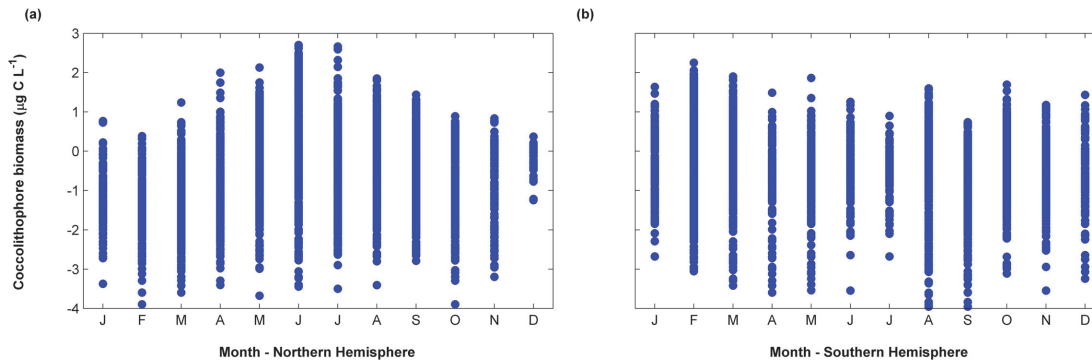
Fig. 6. Seasonal distribution of coccolithophore biomass data for **(a)** Northern Hemisphere and **(b)** Southern Hemisphere.
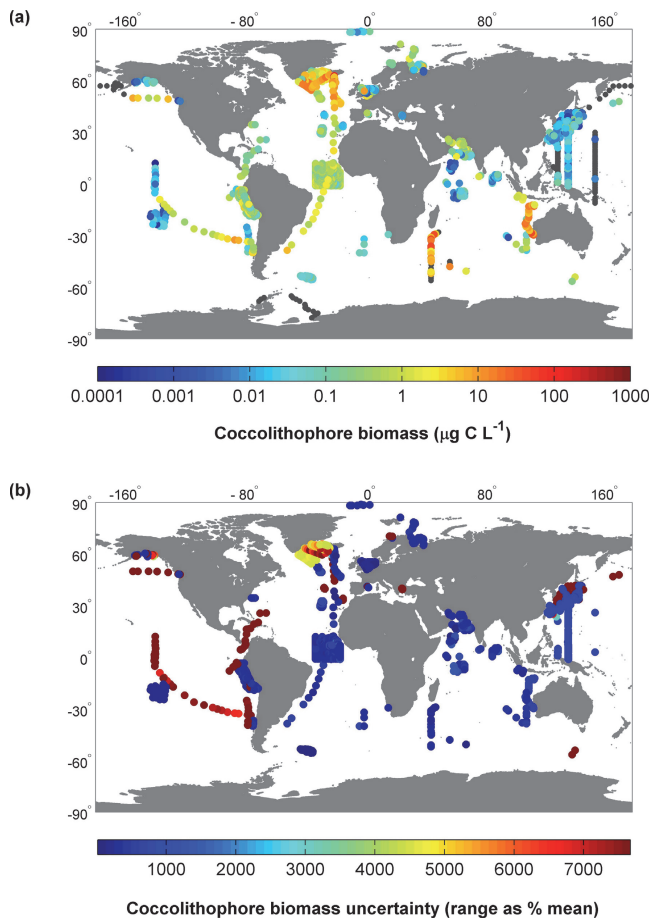
Fig. 7. (a) Surface (0–5 m) mean coccolithophore biomass ($\mu g\, C\, l^{-1}$) and **(b)** range of uncertainty in cell biomass estimates (% of the mean) due to uncertainty in cell size.